JOM, Vol. 67, No. 11, 2015
DOI: 10.1007/s11837-015-1588-0

Modeling and Simulation of the MIDREX Shaft Furnace: Reduction, Transition and Cooling Zones

ALIREZA SHAMS[1,3] and FAEGHEH MOAZENI[2]

1.—Department of Chemical Engineering, McGill University, Montreal, QC H3A 0C5, Canada. 2.—Department of Civil and Environmental Engineering and Construction, University of Nevada, Las Vegas, NV 89154, USA. 3.—e-mail: alireza.shams@mail.mcgill.ca

Metallic iron used in steel industries is mostly obtained from a direct reduction process. The focus of this study is to simulate the furnace of the MIDREX technology. MIDREX technology which is the most important gas-based direct reduced iron (DRI) process in the world, includes reduction, transition and cooling zones. The reduction zone considered as a counter current gas–solid reactor produces sponge iron from iron ore pellets. The transition zone has sufficient height to isolate the reduction zone and cooling zone from each other and the cooling zone cools the solid product down to around 50°C. Each zone has a system of reactions. Simultaneous mass and energy balances along the reduction zone lead to a set of ordinary differential equations with two points of boundary conditions. The transitions and cooling zone are investigated at the equilibrium condition leading to a set of algebraic equations. By solving these systems of equations, we determined the materials concentration, temperature, and pressure along the furnace. Our results are in a good agreement with data reported by Parisi and Laborde (2004) for a real MIDREX plant. Using this model, the effect of reactor length and cooling gas flow on the metallization and the effect of cooling gas flow on the outlet temperature of the solid phase have been studied. These new findings can be used to minimize the consumed energy.

Nomenclature

A_p	pellet external area (m^2)
C	reactor gas concentration (mol/m^3)
C_p	heat capacity (j/mol K)
D	diffusion constant
h	global heat transfer coefficient (pellets/gas)
k	kinetics constant of the surface reaction
k_g	external mass transfer coefficient (m/s)
L	reduction zone length (m)
M	metalizing percent
M_w	molecular weight
n_p	number of pellets per unit volume
P	pressure (bar-g)
Q_m	molar flow (mol/m^2s)
R	reaction rate
r_0	external radius of the pellet (m)
r_c	radius of unreacted core (m)
T	temperature (°C)
u	velocity (m/s)
X	extent of reaction/extent of reactant conversation (mol/m^3)
z	space variable inside the reactor (m)

Subscripts

g	gas
i, j	counter
in	reactor inlet
n	number of carbon atoms
s1	reactive solid
s2	product solid
v	gaseous reactant

Greek Letter

α	stiochiometric coefficient
ε_{mf}	axial voidage
ρ	density (g/m^3)

INTRODUCTION

The direct reduction is a process for reducing iron ore and producing sponge. There are several technologies, like MIDREX[1] and H.Y.L[2] using the countercurrent shaft furnace to make sponge iron.

(Published online August 21, 2015)

In MIDREX technology, the furnace is a vertical shaft (Fig. 1). A charge of pelletized or lump ore is loaded into the top of the furnace and descends by gravity through the reducing gas. The gas is moved upward passing the ore. Reduction takes place in the central and upper parts of the furnace at a temperature above 900°C. After the reduction zone, there is the transition zone. If the solid phase temperature is high enough, the in-situ reforming reactions can occur.[1] In-situ reforming shows several beneficial functions such as increasing plant productivity and decreasing overall energy consumption. This zone contains sufficient length which separates the reduction zone from the cooling zone gas in order to allow an independent control. The reduced sponge iron is then discharged into the lower part of the furnace and cooled down to about 50°C prior to release to the atmosphere. This type of furnace provides the efficient gas–solid contact and heat exchange resulting in maximum productivity per unit furnace volume and minimum consumption of fuel per ton of reduced iron.[3]

Modeling of widely used industrial processes can help us understand the effect of changes in operation conditions when the experiments are expensive and time consuming.[4] In recent years, modeling and simulation of MIDREX process has attracted a lot of attentions. Previous studies have tried to model the reduction furnace[5] yet most of the models have been limited to one zone only.

Modeling of the reduction zone has also been the topic of several studies. In order to simplify the calculations associated with the gas–solid conditions in the reduction furnace, a counter-current flow has been used.[3] Munro and Amundson,[6] Amundson[7] and Siegmund et al.[8] used a linear function of the solid temperature in moving bed solid–gas reactors to estimate the reaction rate. The accuracy and applicability of this model are limited to a small range of temperatures.[3] Heat generation in a steady-state reactor has been studied by Schaefer et al.[3,9] using a step function of the heat balance. Yoon et al.[10] developed a model for a Lurgi type reactor used in the carbon gasification by considering the same temperature in both solid and gas phases and the shrinking unreacted core model for the solid particle. The same system has been studied by Amundson and Arri[3,11] by considering different temperatures in both phases. Parisi and Laborde[3] analyzed operating conditions affecting metallization by using an unreacted core model for the solid particles, in a counter-current moving bed reactor. Their model is stronger compared to similar ones. The model developed by Rao and Pichestapong for a reactor carry out the reduction of iron mineral. This model considers the controlling step as the mass transfer of the gaseous reactants in the product solid layer, but it doesn't take into account the heat transfer and assumes a linear profile for the temperature with the reactor length.[3] Unlike the reduction zone, each of transition and cooling zones has been simulated separately by several studies. For instance, Alamsari et al.[12] formulated the heat and mass transfer equations to estimate the temperature and concentration of gas and solid phases.

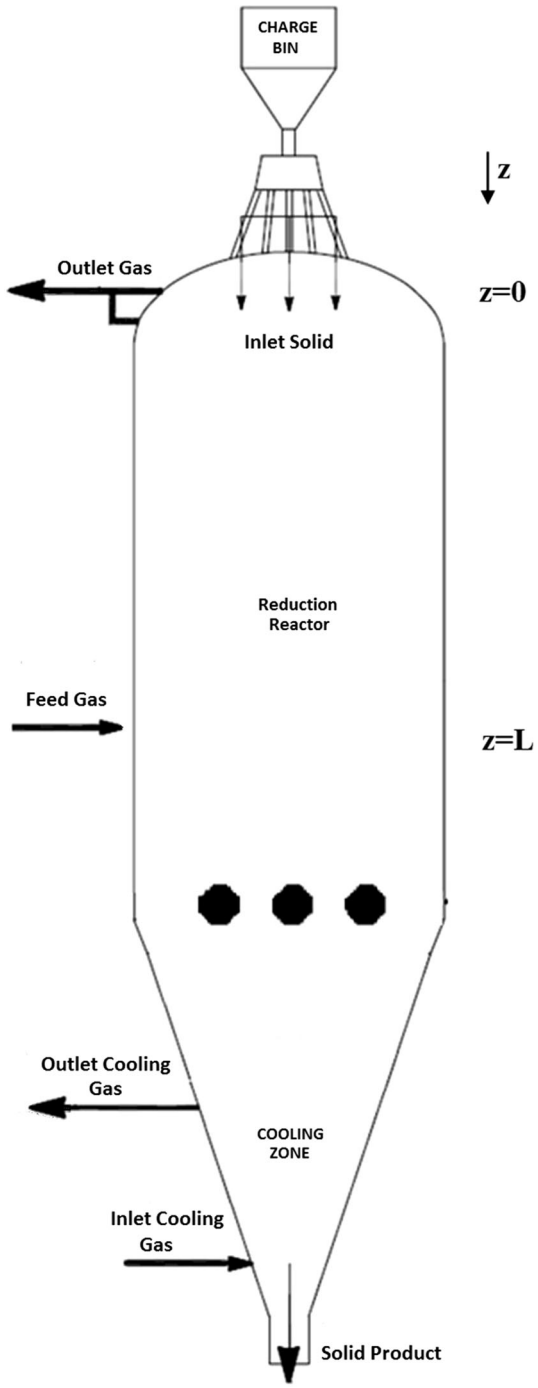

Fig. 1. Shaft furnace of MIDREX process (adapted from Ref. 3).

The aim of this work is to model and simulate all parts of the MIDREX reduction furnace including a solid–gas countercurrent moving bed reactor, transition and cooling zones. In this system, iron ore pellets are reduced by the use of CO and H_2 as reducing gases and then they pass the transition

and cooling zones. All the results are verified using industrial data[3] and the effect of some of the operating conditions are studied.

MATHEMATICAL MODEL

Reduction Zone

In order to model the MIDREX shaft furnace (Fig. 1), based on Parisi and Laborde,[3] the following assumptions are considered:

(a) The iron ore pellet consumption is estimated by the unreacted shrinking core model. This approximation has been used in several studies.[13]
(b) Compared to the diffusional resistance inside the porous solid, mass and heat transfer resistances through the film around the solid particle are negligible ($k_g \gg D/2/r_0$).
(c) Only steady-state operating conditions is considered.
(d) High gas flow rate in the reactor, results in turbulence regime. Under this situation, inertial effects are dominant; so neither axial nor radial dispersion is considered.[14]

The reaction system studied in reduction zone is as following:

$$Fe_2O_3 + H_2 \rightarrow 2FeO + H_2O$$
$$FeO + H_2 \rightarrow Fe + H_2O \quad \text{(R1)}$$
$$Fe_2O_3 + CO \rightarrow 2FeO + CO_2$$
$$FeO + CO \rightarrow Fe + CO_2 \quad \text{(R2)}$$

It must be noted that every couple reactions are considered as a single reaction by using this assumption that all of Fe_2O_3 changes to FeO. The extent of reactions is defined in terms of concentration as:

$$C_j = C_j^0 + \sum_i \beta_j^i X_i \quad (1)$$

Using the above equation, it can be written for the gaseous phase,

$$X_1 = C^0_{H_2} - C_{H_2} \quad (2)$$

$$X_2 = C^0_{CO} - C_{CO} \quad (3)$$

and for the solid phase,

$$X_s = C^0_{FeO} - C_{FeO} \quad (4)$$

Considering the unreacted shrinking core model, we can relate the radius of the unreacted core (r_c) to the solid conversion (X_s) through Eq. 5,[3]

$$r_c = \left(r_0^3 - \frac{X_3 M_w}{4 n_p \pi \rho}\right)^{1/3} = r_0(1 - X_s)^{1/3} \quad (5)$$

where r_0 is the external radius of the pellet, n_p the number of pellets per unit reactor volume, ρ and M_w are the density of the reactive solid and the molecular weight, respectively.

Under the above assumptions (a-e), the mass balances for a steady-state counter current moving bed reactor can be written as:

$$u_g \frac{dX_1}{dz} + n_p R_1(X_1, X_s) = 0 \quad (6)$$

$$u_g \frac{dX_2}{dz} + n_p R_2(X_2, X_s) = 0 \quad (7)$$

$$u_s \frac{dX_s}{dz} + n_p(R_1(X_1, X_s) + R_2(X_2, X_s)) = 0 \quad (8)$$

where u_g and u_s are the gas and solid velocities in the reduction zone and R_i is the reaction rate per pellet, respectively. The energy balances are:[3]

$$\frac{dT_g}{dz} - \frac{n_p A_p h(T_s - T_g)}{Q_{mg} C_{pg}(X_1, X_2, T_g)} = 0 \quad (9)$$

$$\frac{dT_s}{dz} - \frac{n_p}{Q_{ms}(X_s) C_{ps}(X_s, T_s)} \left[A_p h(T_s - T_g) - \sum_i \Delta H_i(T_s) R_i(X_i, X_s, T_s)\right] = 0 \quad (10)$$

The boundary conditions for Eqs. 6 to 10 are:[3]

$$at\ z = L : X_1 = X_2 = 0, \text{ and } T_g = T_g^{in} \quad (11)$$

$$at\ z = 0 : X_s = 0, \text{ and } T_s = T_s^{in} \quad (12)$$

Using the shrinking core model for the solid pellet; the corresponding reaction rate expression per pellet is given by:[3]

$$R_v = \frac{-4\pi r_c^2 C_v}{\left(\frac{1}{k_v} + \frac{r_c}{D_v} - \frac{r_c^2}{r_0 D_V}\right)} \quad (13)$$

where v = 1,2 denotes H_2 and CO, respectively. It must be noted that this model is based on an irreversible kinetics, which means that the validity of the simulation is limited to the conditions in which the gas compositions are far from equilibrium in reduction zone.

The solid molar flow (Q_{ms}) is related to shrinking core radius by Eq. 5, so it can be evaluated using following expression:

$$Q_{ms} = Q^0_{ms} \frac{\left[\frac{r_c^2}{2}\frac{\rho_{s1}}{M_{ws1}} + (r_0^3 - r_c^3)\rho_{s2}/M_{ws2}\right]}{\left[r_c^2 \frac{\rho_{s1}}{M_{ws1}} + (r_0^3 - r_c^3)\rho_{s2}/M_{ws2}\right]} \quad (14)$$

where s_1 and s_2 denote FeO and Fe, respectively. The solid specific heat is calculated using:

$$C_{Ps} = \frac{\left[C_{ps1}\rho_{s1}r_c^3 + C_{ps2}\rho_{s2}\left(r_0^3 - r_c^3\right)\right]}{\left[\rho_{s1}r_c^3 + \rho_{s2}\left(r_0^3 - r_c^3\right)\right]} \quad (15)$$

This equation considers the C_p weighted average of reactive solid (s_1) and product solid (s_2) for any state of transformation given by the unreacted radius (r_c). Heat transfer coefficient (h) is obtained from Chilton and Colburn correlation,[15] used for packed bed reactors (neglecting the resistance in the gaseous film),

$$h = \frac{\mathrm{Pr}^{2/3}}{C_{Pg}Q_{mg}} \quad (16)$$

where Pr is the Prandtl number which is estimated locally based on the temperature and concentration. The model differential equations with boundary conditions are solved numerically using Runge–Kutta-Gill method.[16]

Transition Zone

In this zone, the effect of natural gas is closely related to the free carbon formation. Motlagh[17] studied the effect of gas flow on simultaneous carburization and reduction of iron ore and showed that carbon deposition did not occur in the absence of iron or without a catalyst, irrespective of the gas flow or heating rate of the gas mixture. In the presence of metallic iron, the rates of reduction and carbon deposition can be related to the gas flow rate. The main reactions in this zone are:[17]

$$C_nH_{2n+2} + 3n\mathrm{Fe} \rightarrow n\mathrm{Fe_3}C + (n+1)H_2$$
$$nFe_3C \rightarrow 3nFe + nC \quad (\mathrm{R3})$$

It is assumed that all of hydrocarbons which are heavier than methane are decomposed on the iron powder. The yield of following reactions for methane is related to the temperature and the amount of natural gas. The mass balance for free carbon and hydrogen are mentioned as

$$C_C = n_p n R_3\left(C_{C_nH_{2n+2}}, T_s\right) \quad (17)$$

$$C^0_{H_2} - C_{H_2} = -(n+1)n_pR_3\left(C_{C_nH_{2n+2}}, T_s\right) \quad (18)$$

where C_c is the concentration of free carbon. The remained molecules of natural gas are mixed to reducing gas and move to the top of the furnace. Because the amount of methane in comparison with the amount of reducing gas is very small (about 1%), the changes in temperature profile for both gas and solid flow are very small.[17] It will be calculated as a function of heat of reaction.

If the solid phase temperature is high enough (above 900°C), the in-situ reforming will occur. In this condition, the natural gas reacts with CO_2 and H_2O to produce H_2 and CO. The following reactions are expected:[17]

$$\mathrm{CH_4 + CO_2 \rightarrow 2CO + 2H_2} \quad (\mathrm{SR1})$$
$$\mathrm{CH_4 + H_2O \rightarrow CO + 3H_2} \quad (\mathrm{SR2})$$

The mass and energy balance equations can be stated as

$$C^0_{\mathrm{CO}} - C_{\mathrm{CO}} = -2R_{S1}\left(C_{\mathrm{CH_4}}, C_{\mathrm{CO_2}}, T_g\right) - R_{S2}\left(C_{\mathrm{CH_4}}, C_{\mathrm{H_2O}}, T_g\right) \quad (19)$$

$$C^0_{\mathrm{H_2}} - C_{\mathrm{H_2}} = -2R_{S1}\left(C_{\mathrm{CH_4}}, C_{\mathrm{CO_2}}, T_g\right) - 3R_{S2}\left(C_{\mathrm{CH_4}}, C_{\mathrm{H_2O}}, T_g\right) \quad (20)$$

$$C^0_{\mathrm{H_2O}} - C_{\mathrm{H_2O}} = R_{S2}\left(C_{\mathrm{CH_4}}, C_{\mathrm{H_2O}}, T_g\right) \quad (21)$$

$$C^0_{\mathrm{CO_2}} - C_{\mathrm{CO_2}} = R_{S1}\left(C_{\mathrm{CH_4}}, C_{\mathrm{CO_2}}, T_g\right) \quad (22)$$

$$C^0_{\mathrm{CH_4}} - C_{\mathrm{CH_4}} = R_{S1}\left(C_{\mathrm{CH_4}}, C_{\mathrm{CO_2}}, T_g\right) + R_{S2}\left(C_{\mathrm{CH_4}}, C_{\mathrm{H_2O}}, T_g\right) \quad (23)$$

$$\Delta T_s = \frac{A_p h\left(T_s - T_g\right) - \sum_i \Delta H_{Si}(T_s)R_{Si}(T_s)}{Q_{ms}(X_s)C_{ps}(X_s, T_s)} \quad (24)$$

Cooling Zone

The cooling process of sponge iron product in the cooling zone will also produce free carbon (C) in the product. Around 1% of cooling gas usually slips, and reacts with solid pellets came from reduction zone. In this zone, free carbon is formed as a result of methane and other hydrocarbons cracking. Water gas shift reaction also occurs in the cooling zone. The reaction system in cooling zone is as following:

$$C_nH_{2n+2} \rightarrow nC + (n+1)H_2\ (n>1) \quad (\mathrm{R3})$$
$$\mathrm{H_2O + CO \leftrightarrow H_2 + CO_2} \quad (\mathrm{R4})$$
$$\mathrm{CH_4 + H_2O \leftrightarrow CO + 3H_2} \quad (\mathrm{R5})$$

The equations are formulated by assuming:[12]

(a) The system has reached an equilibrium condition.
(b) Heat loss trough the wall of the reactor is neglected.
(c) Ethane, propane and other heavier hydrocarbons are decomposed completely.

By considering above assumptions, heat and mass transfer equations can be stated as:

$$C^0_{\mathrm{CH_4}} - C_{\mathrm{CH_4}} = n_pR_3(C_{\mathrm{CH_4}}, T_s) + R_5(C_{\mathrm{CH_4}}, C_{\mathrm{H_2O}}, T_g) \quad (25)$$

$$C^0_{\mathrm{CO}} - C_{\mathrm{CO}} = R_4\left(C_{\mathrm{H_2O}}, C_{\mathrm{CO}}, T_g\right) - R_5(C_{\mathrm{CH_4}}, C_{\mathrm{H_2O}}, T_g) \quad (26)$$

$$C^0_{\mathrm{H_2}} - C_{\mathrm{H_2}} = -(n+1)n_pR_3\left(C_{C_nH_{2n+2}}, T_g\right) - R_4(C_{\mathrm{H_2O}}, C_{\mathrm{CO}}, T_s) - 3R_5(C_{\mathrm{CH_4}}, C_{\mathrm{H_2O}}, T_g) \quad (27)$$

$$C^0_{H_2O} - C_{H_2O} = R_4(C_{H_2O}, C_{CO}, T_g) + R_5(C_{CH_4}, C_{H_2O}, T_g) \quad (28)$$

$$\Delta T_s = \frac{A_p h(T_s - T_g) - \sum_i \Delta H_i(T_s) R_i(T_s)}{Q_{ms}(X_s) C_{ps}(X_s, T_s)} \quad (29)$$

$$\Delta T_g = \frac{A_p h(T_s - T_g)}{Q_{cg}, Cp_{cg}} \quad (30)$$

where *cg* denotes the cooling gas. It must be noted that the calculation of both of transition and cooling zone is done at the equilibrium condition.

Estimation of Pressure Drop

The estimation of pressure drop for a reduction furnace is not easy because its operation is not completely compatible to a fixed bed or a fluidized bed. We studied various numbers of the correlations reported by several researchers[18–21] to find a suitable relationship for estimating pressure drop for the MIDREX furnace. The following equation was used to calculate the pressure along the reactor:

$$\frac{dP}{dz} = 150\left[\frac{(1-\varepsilon_{mf})^2}{\varepsilon^3_{mf}\left(\frac{\mu_g u_g}{r_c^2}\right)}\right] + 1.95\left[\frac{1-\varepsilon_{mf}}{\varepsilon^3_{mf}\left(\frac{\mu_g u_g^2}{r_c}\right)}\right] \quad (31)$$

where ε_{mf} is axial voidage estimated by following correlation:[22]

$$\varepsilon_{mf} = 0.453 z^{0.119}\left(\mathrm{Re}_g/\mathrm{Re}_s\right)^{0.076} \quad (32)$$

where Re_g and Re_s are gas phase Reynolds number and solid phase Reynolds number.

RESULTS AND DISCUSSION

Before solving the model equations, all of the parameters were extracted from reliable references. Values of reaction enthalpies (ΔH) and specific heats (Cp) were taken from NIST.* The reaction kinetics for R1 and R2 is obtained from Ref. 3 and the reaction kinetics and equilibrium constants for SR1, SR2, R3, R4 and R5 are obtained from Refs. 17, 23 The physical properties for both of gas and solid phases are obtained from Ref. 15 The information of kinetic constants and diffusion coefficients is given in Table I. The operating conditions of the reduction zone of Gilmore, a MIDREX plant,[3] are given in Table II and comparison of the plant data with our model is given in Table III.

The data for other zones (transition and cooling) obtained from Ref. 12 Some of data, which are not reported by references, were determined using our model. Table III presents the results of the model predictions in comparison with the industrial plant data. This Table shows that the results of our model are in a good agreement with the plant data. It means presented model have a good reliability to predict the operation of a reduction furnace.

Because carbon is a major component in further steel process, increasing the amount of Carbon can be helpful. The model shows with about 6% Methane in reducing gas flow, solid product contains around 1.4% Carbon.

A small part of cooling gas flows upward and mixed with the reducing gas. During the cooling process, which decreases the temperature of solid to around 56°C, some reactions occur. This can prove why the outlet cooling gas has a lower flow rate, 10,758.8 Nm^3/h, than the inlet cooling gas flow, 11,800 Nm^3/h. The composition of outlet gas is different from the one of inlet cooling gas and all of heavy hydrocarbon is decomposed to Carbon and Hydrogen.

Figure 2 shows the profile of gas pressure along the reduction zone. The Top (outlet) gas pressure is affected by both of gas and solid flow rates. Because the reducing gas flows upward, the only effective length on pressure drop is the length of reduction zone. It can be seen that by increasing the length of the reactor, the pressure increases. For a 10 m reduction zone, we reach 1.4 bar pressure.

Figure 3 shows the profile of solid phase temperature along the reduction zone. It can be seen that the temperature of solid phase increases rapidly near the inlet zone. As the solid phase enters the reactor, it faces with a large amount of hot gas, so its temperature increases rapidly. In fact, this rapid change is necessary for occurring reactions. The reduction zone needs to work on a high temperature to obtain maximum metallization. Around 2 meters far from the inlet zone (25% of reactor depth) solid reaches a rather stable temperature which changes smoothly to the end of reduction zone. Solid particles enter the transition zone with a temperature around 920°C that doesn't change obviously along this part of the furnace. The flow of cooling gas and its inlet temperature affects the temperature of solid products.

Figure 4 shows the variation of mole fraction of gas phase components versus the reduction zone length. Although some of reactions which occur in transition and cooling zones affect the concentration of components, the most of changes occur along the reduction zone. It is obvious that the different concentrations used in the reducing gas allow both CO and H_2 act simultaneously throughout the entire reactor, removing the same amounts of oxygen. Also, it is clear that the CO is a better reducer than the H_2 because with smaller concentrations of CO similar efficiency are achieved. It is observed that molar fractions of gases within the reactor, like the temperature, tend to be uniform as the length grows.

*http://webbook.nist.gov/chemistry/.

Table I. Kinetics constants and Diffusion coefficients[3,17,23,24]

Parameters	Equation	Unit
k_1	0.00225exp(−1482.35/8.314/T)	m/s
k_2	0.00650exp(−2846.98/8.314/T)	m/s
k_3	*Assume 100% convergence for hydrocarbon heavier than Methane and for Methane:* 0.00196exp (−17,600/8.314/T)	m/s
k_4	12.19exp(−671,300/8.314/T)	m/s
k_5 and k_{S2}	20,115.6exp(−23,700/8.314/T)	$(mol/m^3)^{0.5}/s$
k_{S1}	21890exp(−240,100/8.314/T)	$(mol/m^3)^{0.5}/s$
D_1	$1.467 \times 10^{-10} \times T^{1.75}$	m^2/s
D_2	$3.828 \times 10^{-11} \times T^{1.75}$	m^2/s

Table II. Operating conditions of a MIDREX Plant[2,12]

Feed gas	
Flow rate (Nm^3/h)	53,863
Temperature (°C)	930
Pressure (barg)	1.4
Composition (%)	
H_2	52.58
CO	29.97
H_2O	4.65
CO_2	4.80
$CH_4 + N_2$	8.1
Inlet cooling gas	
Flow rate (Nm^3/h)	11,800
Temperature (°C)	43
Composition (%)	
H_2	21.36
CO	3.1
H_2O	1.96
CO_2	3.4
CH_4	67.8
N_2	1.86
C_2H_6	0.23
C_3H_8	0.143
Solid	
Production (tons/h)	26.4
Average diameter (mm)	10
Temperature (°C)	35
Composition (%)	
Fe_2O_3	95 (assumption)
Gangue	5 (assumption)
Reactor	
Length (m)	9.75
Average diameter (m)	4.26

Figure 5 shows the effect of reactor depth on metallization. The metallization percent is defined as follows:

$$M(\%) = \frac{\text{Fe}}{\text{Total Fe}(\text{Fe} + \text{FeO})} \times 100 \qquad (33)$$

We ignore other oxides such as SiO_2, Al_2O_3, etc. in pellets. The fact that 100% of metallization is never reached in practice in this reactor not only because of a mass transfer control, but because the difficulty in reducing the other oxides. In normal operating condition, estimated metallization is 92.35% for 26.4 t/h product. This means that minimum feed for solid gas must be 37.4 t/h. It can be seen that the whole reactor length is used efficiently for the transformation of the solid and the solid is transformed completely before arriving to the outlet zone but the residence time would be greater than the essential and the production would be lower than the maximum production capacity of the plant.

Figure 6 shows if the flow of cooling gas increases, the outlet temperature of solid product decreases. The temperature of solid cannot become less than the inlet temperature of cooling gas; so there is an optimum flow for cooling that is economical. In our case, the inlet temperature of cooling gas is around 40°C and the optimal cooling gas flow rate is around 11,800 Nm^3/h. Increasing the flow rate to 13,000 Nm^3/h deceases the solid temperature only from 50 to around 45.

CONCLUSION

The whole part of the shaft furnace of MIDREX direct reduction technology, the reduction, transition and cooling zone, was simulated. In this study, mass and energy balance for each phase in each zone were solved. The equation system allows us to know the evolution of several variables throughout the reactor. Our model showed the logical results which have a similar procedure like what reported by Parisi and Laborde[3] and Alamsari et al.[12] for a MIDREX plant. The proposed model allows studying different operation regimes, for example, the effect of natural gas and cooling gas flow. If the flow of natural gas increases, the production of Carbon increases. In the cooling zone, the more flow of cooling gas leads to cooler solid product, but in this condition, the metallization decrease in a small value. It is observed if metallization increase, the production must decrease and it is not advisable. Alternatively, if the production increases, the metallization decreases. In a normal operation condition, the plant produces 37.4 t/h products with 92.36% of metallization. The present of Methane

Table III. Comparison of the Gilmore data with model prediction

	Model results	Plant data	Error (%)
Top (outlet) gas			
Flow rate (Nm^3/h)	60,891.5	No data	–
Temperature (°C)	474.82	No data	–
Pressure (barg)	0.53	No data	–
Composition (dry base) (%)			
H_2	37.96	37	2.52
CO	19.44	18.9	2.85
CO_2	17.54	16.1	8.94
H_2O	18.04	21.2	14.9
$CH_4 + N_2$	7.02	8.6	18.37
Outlet cooling gas			
Flow rate (Nm^3/h)	10,758.8	10,607	1.43
Temperature (°C)	455.4	460	1.00
Composition (%)			
H_2	21.63	24.26	10.84
CO	3.44	2.1	63.81
H_2O	1.98	1.96	1.01
CO_2	4.14	4.39	5.69
CH_4	66.65	65.66	1.50
N_2	2.16	1.85	16.75
C_2H_6	0	No data	–
C_3H_8	0	No data	–
Solid			
Temperature before reduction zone (°C)	915.14	930	1.62
Temperature after reduction zone (°C)	56.12	58	3.24
Composition (%)			
Fe	83.56	No data	–
FeO	8.87	No data	–
Carbon	1.42	2	29
Ganuge	6.07	6.3	3.65
Production (tons/h)	26.48	26.4	0.3
Required solid feed (tons/h)	37.3	No data	–
Metallization percent (%)	92.36	93	0.69

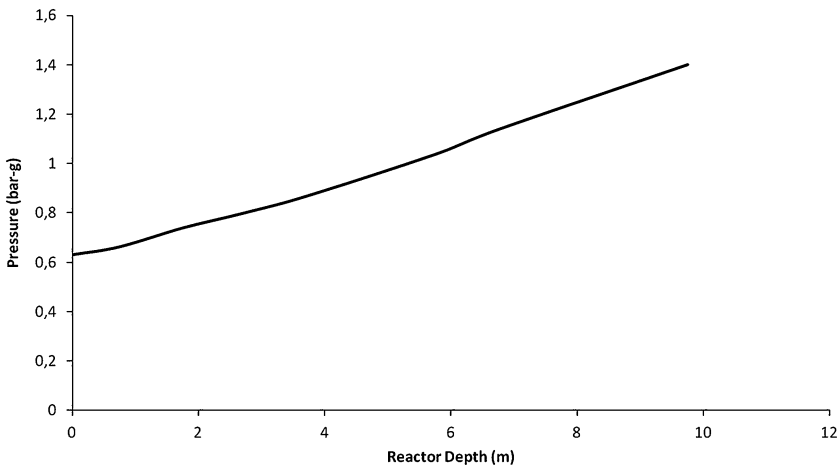

Fig. 2. Profile of gas pressure along the reduction zone.

results in producing Carbon. The final product contains about 1.4% Carbon. The cooling gas that cools the solid to around 56°C helps production of Carbon and small part of it flows upward and mixed with the reducing gas. The profile of mole fractions, solid temperature and pressure were studied. It is obvious that the different concentrations used in the reducing gas allow both CO and H_2 act

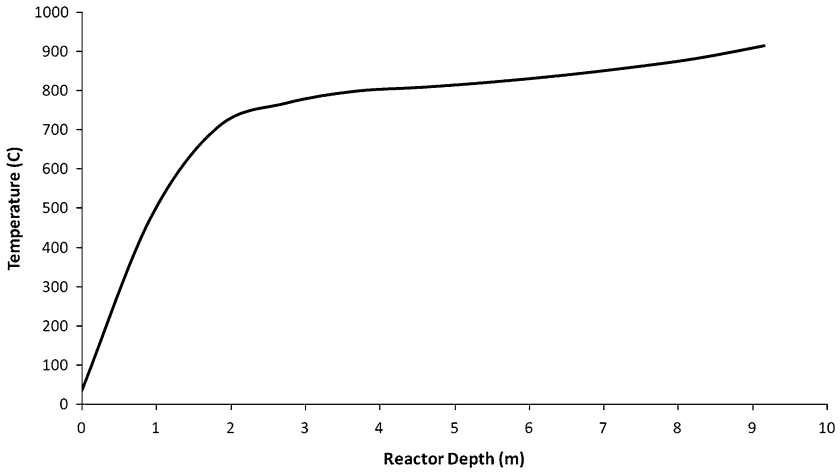

Fig. 3. Profile of solid phase temperature along the reduction zone.

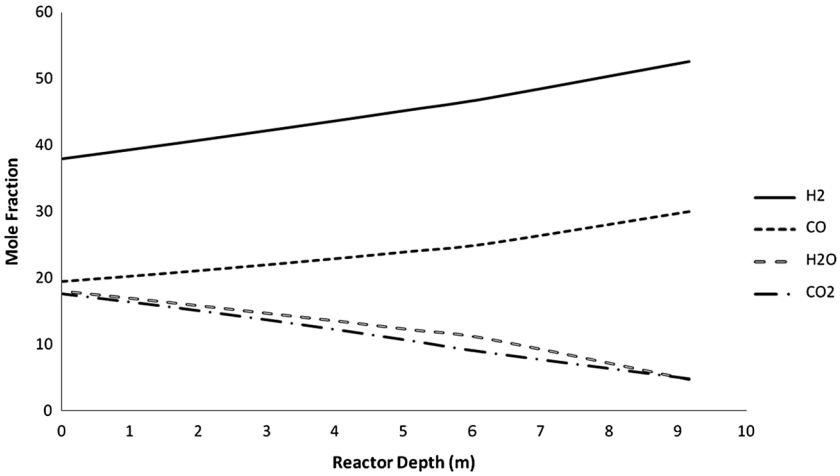

Fig. 4. Variation of mole fraction of gas components versus changing in reactor depth.

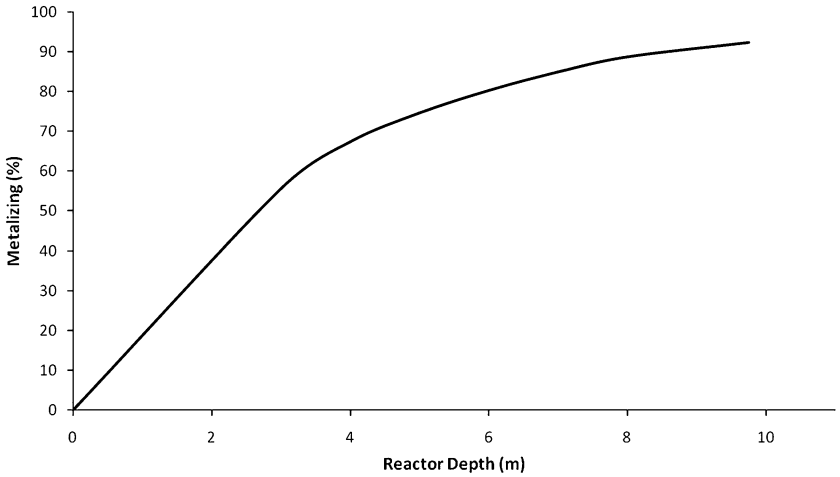

Fig. 5. The effect of reactor length on the metallization.

simultaneously throughout the entire reactor, removing the same amounts of oxygen. The pressure drop for the 9.75 m length of reduction zone is about 0.87 bar. Because the gas flow is upward, the only effective length on pressure drop is the length of reduction zone.

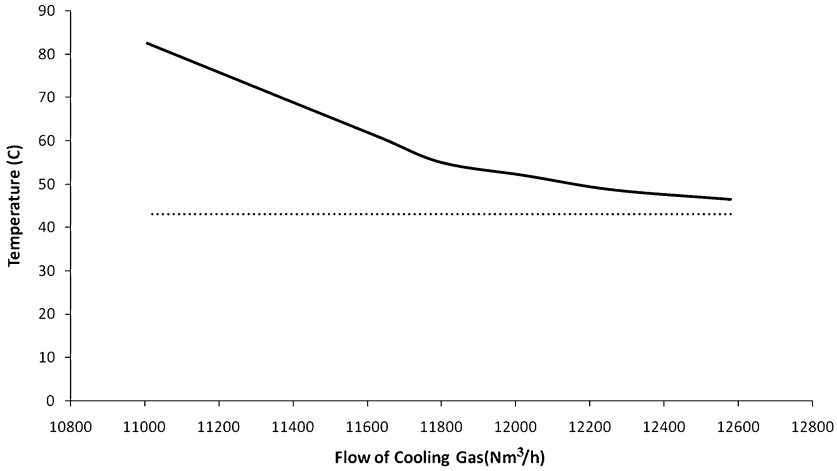

Fig. 6. The effect of cooling gas flow on the outlet temperature of solid phase.

REFERENCES

1. MIDREX Tech. (2009). http://www.midrex.com/.
2. Hytempsys, Chapter 1 (2009).http://www.energiron.com/Tour/HYLDRMinimillQTVRtour.
3. D.R. Parisi and M.A. Laborde, *Chem. Eng. J.* 104, 35 (2004).
4. A. Shams, A.M. Dehkordi, and I. Goodarznia, *Energy Fuels J.* 22, 570 (2008).
5. K.O. Yu and P.P. Gillis, *Metall. Trans. B* 128, 111 (1981).
6. W.D. Munro and N.R. Amundson, *Ind. Eng. Chem.* 42, 1481 (1950).
7. N.R. Amundson, *Ind. Eng. Chem.* 48, 26 (1956).
8. C.W. Siegmund, W.D. Munro, and N.R. Amundson, *Ind. Eng. Chem.* 48, 43 (1956).
9. R.J. Schaefer, D. Vortmeyer, and C.C. Watson, *Chem. Eng. Sci.* 29, 119 (1974).
10. H. Yoon, J. Wei, and M.M. Denn, *AIChE J.* 24, 885 (1978).
11. N.R. Amundson and L.E. Arri, *AIChE J.* 24, 87 (1978).
12. B. Alamsari, S. Torii, Y. Bindar, and A. Trianto, *Proceeding of International Conference on Computer Engineering and Applications ICCEA in Indonesia* (2010), pp. 479–483.
13. E. Kawasaki, J. Sanscrainte, and T.J. Walsh, *AIChE J.* 8, 48 (1962).
14. C.P. La Singh and D.N. Saraf, *Ind. Eng. Chem. Process Des. Dev.* 18, 364 (1979).
15. R.H. Perry and D.W. Green, *Perry's Chemical Engineer's Handbook*, 7th ed. (New York, NY: Mc. Graw-Hill, 1999).
16. R.G. Rice and D.D. Do, *Applied Mathematical and Modeling for Chemical Engineers* (New York, NY: John Wily & Sons, 1995).
17. M. Motlagh, *Ironmaking Steelmaking* 21, 291 (1994).
18. G.K. Roy and P. Sen Gupta, *Ind. Eng. Chem. Proc. Des. Dev.* 13, 219 (1974).
19. G.K. Roy and K.J.R. Sarma, *IE (I) J.-CH.* 57, 122 (1977).
20. K. Taylor, A.G. Smith, S. Ross, and M. Smith, *Second International Conference on CFD in the Minerals and Process Industries CSIRO*, Melbourne, Australia (1999), pp. 273–280.
21. P. Guimard, D. McNerny, E. Saw, and A. Yang, *Pressure Drop for Flow through Packed Beds*, (Transport Process Laboratory, Carnegie Mellon University, 2004) pp. 06–363.
22. D. Acharya, *IE (I) J. MC.* 85, 219 (2005).
23. M.A. Rakib and K.I. Alhumaizi, *Energy Fuels J.* 19, 2129 (2005).
24. O. Karabelchtchikova (A dissertation submitted to faculty of the Worcester Polytechnic Institute, Worcester, MA, USA, 2007).